European Journal of Medicinal Chemistry 141 (2017) 690–702

Contents lists available at ScienceDirect

European Journal of Medicinal Chemistry

journal homepage: http://www.elsevier.com/locate/ejmech

Research paper

Multifunctional iminochromene-2H-carboxamide derivatives containing different aminomethylene triazole with BACE1 inhibitory, neuroprotective and metal chelating properties targeting Alzheimer's disease

Aida Iraji [a], Omidreza Firuzi [a], Mehdi Khoshneviszadeh [a, b], Marjan Tavakkoli [a], Mohammad Mahdavi [c], Hamid Nadri [d], Najmeh Edraki [a, **], Ramin Miri [a, *]

[a] Medicinal and Natural Products Chemistry Research Center, Shiraz University of Medical Sciences, Shiraz, Iran
[b] Department of Medicinal Chemistry, Faculty of Pharmacy, Shiraz University of Medical Sciences, Shiraz, Iran
[c] Endocrinology and Metabolism Research Center, Endocrinology and Metabolism Clinical Sciences Institute, Tehran University of Medical Sciences, Tehran, Iran
[d] Department of Medicinal Chemistry, Faculty of Pharmacy, Shahid Sadoughi University of Medical Sciences, Yazd, Iran

ARTICLE INFO

Article history:
Received 8 May 2017
Received in revised form
25 September 2017
Accepted 27 September 2017
Available online 28 September 2017

Keywords:
Click reaction
BACE1 inhibitor
Metal chelator
Molecular modeling
Neuroprotective assay
Synthesis

ABSTRACT

Alzheimer's disease (AD) is a neurodegenerative disorder known for the presence of amyloid beta plaques resulting from the sequential action of β-secretase and γ-secretase on amyloid precursor protein. We developed and synthesized, through click reactions, a new family of iminochromene carboxamides containing different aminomethylene triazole. The BACE1 inhibition, neuroprotective capacity and metal chelation of these derivatives make them ideal candidates against AD. Most of the synthesized compounds were shown to have potent BACE1 inhibitory activity in a FRET assay, with an IC_{50} value of 2.2 μM for the most potent compound. Moreover, molecular modeling evaluation of these BACE1 inhibitors demonstrates the vital role of the amine and amide linkers through hydrogen bond interactions with key amino acids in the BACE1 active site. Our *in vitro* neuroprotective evaluations in PC12 neuronal cells of Aβ-induced neuroprotection demonstrated promising activity for most of the compounds as neuroprotective agents. Based on our findings, we propose that introduction of a phthalimide substitute on the triazole ring shown to be interesting multifunctional lead compound worthy of further study.

1. Introduction

Alzheimer's disease (AD) is a neurodegenerative disorder and the most common cause of dementia in individuals above the age of 65 [1]. AD is generally characterized by malfunctioning of neurons followed by gradual loss of neurons. The hallmarks of AD are an accumulation of amyloid beta (Aβ) around neurons and neurofibrillary tangles of hyperphosphorylated tau protein within the cells [2]. The amyloidogenic pathway triggered from the breakdown of amyloid precursor protein (APP) by β-secretase (BACE1) followed by γ-secretase cleavage [3], results in the formation of Aβ peptides, which are prone to polymerization into pathological fibrils and other biophysical forms. Various factors, such as mutations of the APP gene, cellular prions [4], hypoxia [5], and environment, may increase β-cleavage relative to α-cleavage, which in turn increases the accumulation of Aβ [6,7]. Based on the above findings, BACE1, a transmembrane aspartic protease comprising two key aspartate residues (Asp32 and Asp228) in the large hydrophobic cleft of the active site, has served as an attractive target for the development of inhibitors against AD [8,9]. Some reported BACE1 inhibitors are peptidic and pseudopeptidic modified molecules [10] such as hydroxyethylene (HE), hydroxyethyleneamine (HEA), carbinamine, acylguanidine, aminoimidazole, and aminoquinazoline [9,11] designed based on the parent structure of APP. Unfortunately, the peptidic inhibitors of BACE1 have poor physicochemical and pharmaceutical properties, such as insufficient oral bioavailability, short serum half-life, or low blood–brain barrier (BBB) penetration.

* Corresponding author.
** Corresponding author.
E-mail addresses: edrakin@sums.ac.ir, najmeh_edraki@yahoo.com (N. Edraki), ramin.miri.15@gmail.com, mirir@sums.ac.ir (R. Miri).

https://doi.org/10.1016/j.ejmech.2017.09.057
0223-5234/

As a consequence, there is an ongoing demand for small molecule BACE1 inhibitor drugs [12].

Many cellular processes in the brain, particularly neuronal activity, require metal ions. Cells have adopted complex mechanisms for maintaining metal ion homeostasis. Disruptions in any of these mechanisms could alter the ionic balance and result in several neurodegenerative disorders including AD [13]. Evidence suggests that bio metals have two distinct roles in the pathophysiology of AD: (i) aggregation of Aβ peptide, and (ii) production of reactive oxygen species induced by Aβ [13–15]. Excess metal ions have been found in Aβ plaques of AD patients' brains [16]. To overcome these neurological disorders, a number of therapeutic strategies aimed at ameliorating or inhibiting Aβ aggregation and induced ROS generation, including the use of metal chelators, are currently being investigated for their potential application in AD therapy [17–19].

The toxic effects of Aβ have been broadly examined. Aβ has been reported to induce oxidative stress-mediated neuronal death [20,21] and apoptosis [22,23]. Recently, efforts have focused on designing new compounds with the potential to protect neural cells from the side effects of Aβ [24,25].

Garino and colleagues reported a new series of compounds containing two fused aromatic rings (naphthyl, coumarin) coupled to aryl piperazine. These compounds demonstrate significant BACE1 inhibition in enzymatic and cell based assays (Scheme 1, compound **1** and **2**) [26,27]. Further structural modifications to identify more potent BACE1 inhibitors led us to imino-2H-chromene and phenylimino-2H-chromen carboxamide moiety coupled to aryl piperazine derivatives as promising BACE1 inhibitors with high potency against BACE1 and cellular production of Aβ in N2a-APPswe cells (Scheme 1, compound **3**) [28]. Following our ongoing research program on finding potent anti-Alzheimer agents [29–31], we aimed to design a novel multi-targeted structure based on our previously reported scaffold, (Scheme 1, compound **3**) [28] with the purpose of optimizing physichochemical properties and anti-Alzheimer potential of this scaffold. To this end, nine candidates of iminochromene-2H-carboxamide derivatives containing different aminomethylene triazole were selected and synthesized based on molecular docking analysis of a small library of designed backbone and further evaluated for their BACE1 inhibitory potential. Protection of neuronal PC12 cells against Aβ-induced damage was examined by 3-(4,5-dimethylthiazol-2-yl)-2,5-diphenyltetrazolium bromide (MTT) reduction assay. Furthermore, metal chelating activity of some compounds was evaluated using a ferrozine-based assay.

2. Results and discussion

2.1. Molecular design and docking study

Designing strategy was carried out in three steps.

1. *Replacement of the piperazine pendant with aminomethylene triazole:* metal therapy is the preferred medical treatment to reduce the toxic effects of metals. Chelators bind to excess metal ions to form complex structures, which are easily excreted from the body. Jiaranaikulwanitch et al. reported tryptoline and tryptamine triazole derivatives as promising metal chelating agent. The metal chelating capability of their compounds could

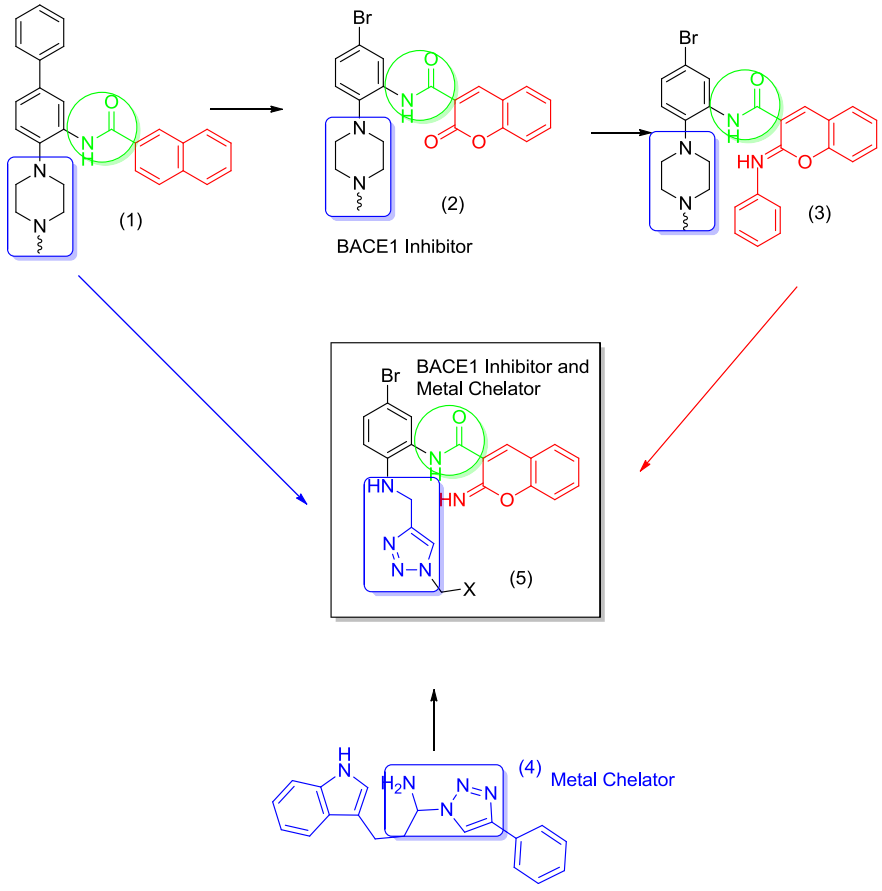

Scheme 1. Molecular hybridization and analogue-based design of imino-2H-chromene carboxamide bearing aminomethylene triazole pendant as novel anti-AD agents.

be attributed to the ione pair of electrons on the nitrogen atom in the amino ethylene linker as well as the nitrogen atom in the triazole ring (Scheme 1, compound **4**) [20]. In the other study 1,2,3-triazole pyridine were reported as bifunctional agent for targeting metal–Aβ species in AD [15]. In this regard, the piperazine linker of previous scaffolds (compounds 1–3) was replaced with the aminomethylene triazole pendant with the aim of introducing a metal chelating moiety and facilitating the interactions with the key catalytic residues of BACE1 active site (Asp32, Asp228). The docking results confirmed that the amine linker demonstrated H-bond interaction with Asp32 in most derivatives. Additional hydrophobic interaction occurs due to the interactions between the amino methylene triazine motif of the ligand and flap loop residues.

2. *Imino-2H-chromen carboxamide containing amide linker* (Scheme 2, *Y part*): arylcarboxamide part was selected based on the molecular docking study of five different fused (hetero) aromatic rings which was previously reported as potential BACE1 inhibitors. Imino-2H-chromen demonstrated favorable pose and oriented toward the S2 pocket of the active site (Table S1). In comparison with the other examined (hetero)aromatic groups, the imino-2H-chromen mostly oriented in the manner that the amide linker of the backbone could involve in H-bound interactions with residues such as Asp228, Gly230 and Thr231. As it is depicted in Table S2, comparison the physicochemical properties of the designed scaffold **5** (LogP = 3.8 with molecular refractivity = 129.6) with the potent derivatives of our previous study [28] (LogP ranging from 5.3 to 7.7 with molecular refractivity ranging from 146.8 to 179.8), demonstrated the superior physicochemical characteristic of newly designed scaffold. These findings prompted us to select compound **5** as promising lead for further optimization and modification. Moreover, the *in vitro* results of our previous study demonstrated that although phenyliminochromene derivatives demonstrated superior BACE1 inhibition in enzymatic assay, they were weakly effective in the cell-based assay. This observation might be attributed to the poor physicochemical properties (such as the low solubility in the culture media and high lipophilicity) of phenyliminochrone derivatives that might compromise its efficiency in the cellular model and hinder their access to their intracellular target. Furthermore, based on computational analysis inappropriate orientation of phenyl fragment in phenyliminochromene derivatives may hinder access and prevent interaction with the Asp228 of the enzyme's active site. The other two heteroaromatic moiety named indole and naphthyl cannot even occupy favorable pockets (Table S1).
3. *Aryl or alkyl motif as X substitute*: computational approaches provided a starting point in the development of new chemical entities. Docking study was performed owing to have limited resources for synthesis, enzymatic and cell based assay. Various substitutions (100 motif) were placed at X positions of the triazole pendant to find the best derivatives for synthesis (Scheme 2). Overall, the X-substituted moieties of the constructed library were selected based on the essential requirement for effective

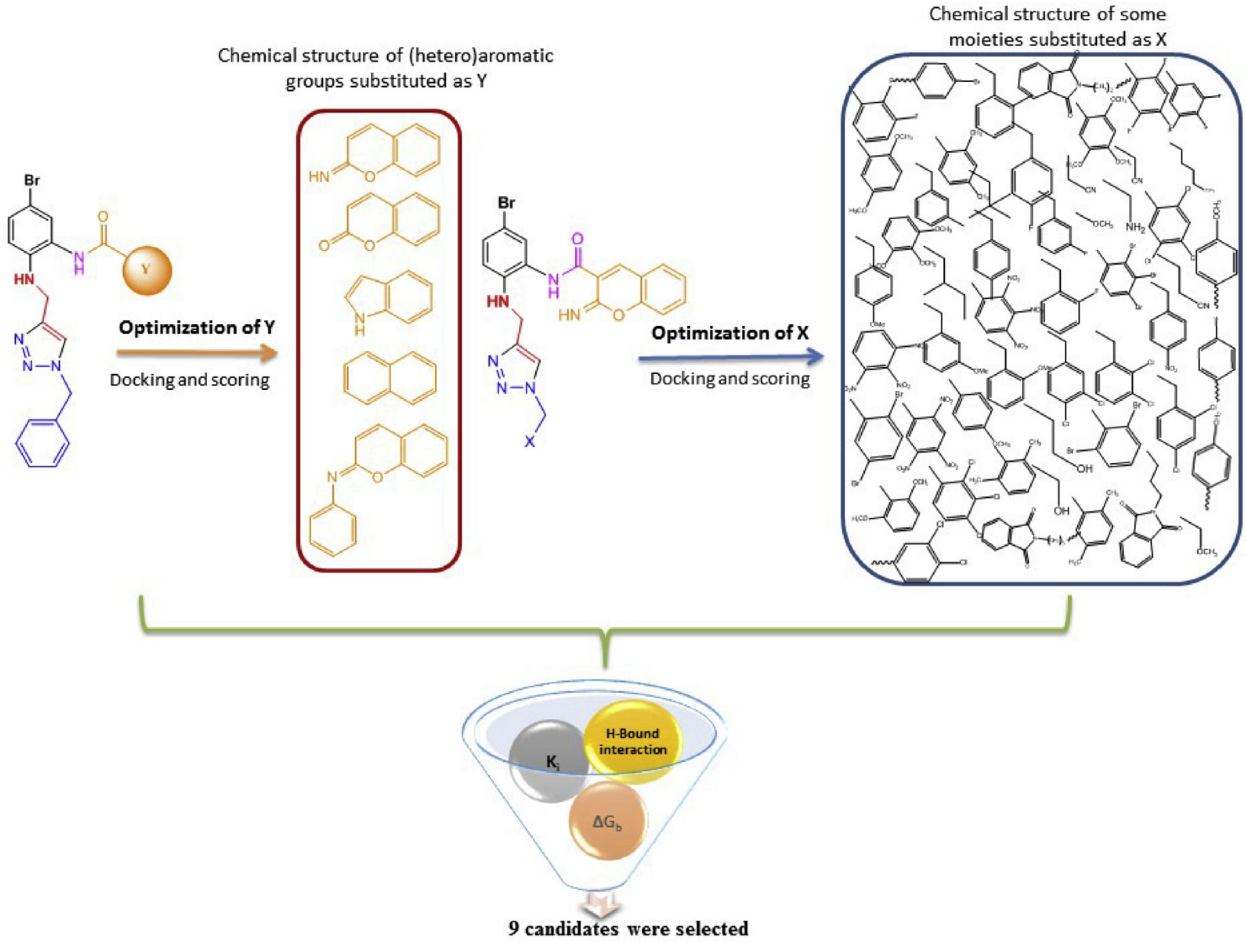

Scheme 2. Schematic representation of molecular design and docking study.

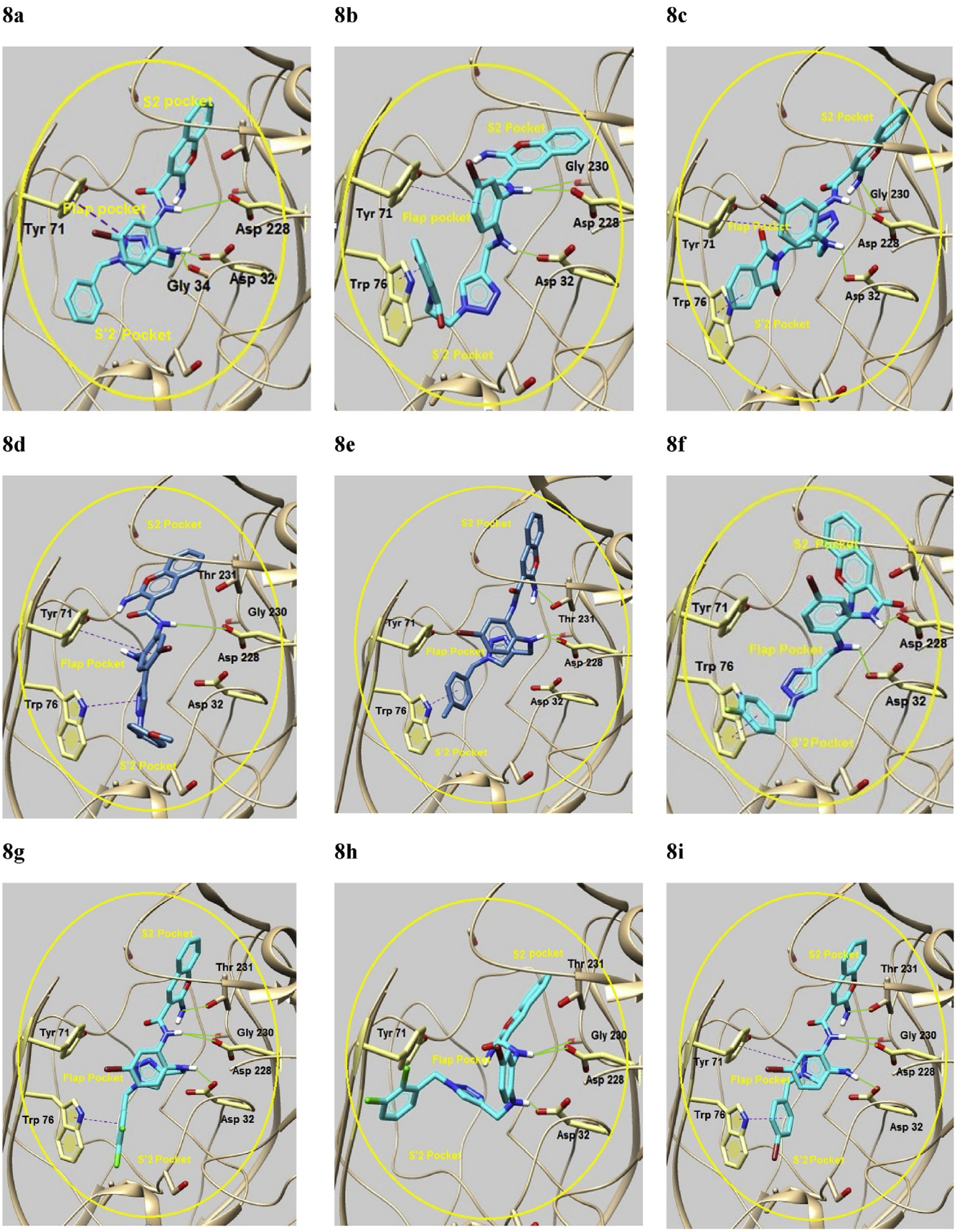

Fig. 1. Binding orientation and interaction of all synthetic compounds in the BACE1 active site. Hydrogen bonds are depicted as green lines. Stacking interactions are demonstrated as purple dashed lines. (For interpretation of the references to colour in this figure legend, the reader is referred to the web version of this article.)

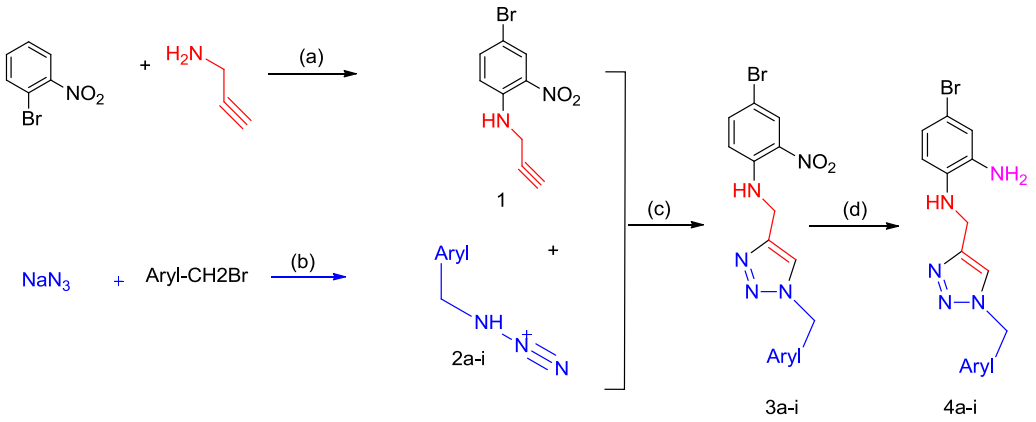

Scheme 3. Protocol, reagents and conditions for the synthesis intermediates **4a-i**. (a) TEA, DMF, reflux, 24 h; (b)NaN_3, TEA t-BuOH/water, rt; (c) $CuSO_4 \cdot 5H_2O$, sodium ascorbate, rt. (d) $Na_2S_2O_6$, Na_2CO_3, MeOH/water, 70 °C, 3–4 h.

binding interaction with BACE1 active site (especially S′2 pocket), feasibility of synthesis and accessibility to chemical reagents. The X substitute attached to the triazole ring is mainly oriented toward the S′2 of active site. It seems that introducing aromatic moieties bearing the appropriate hydrogen bond establishing groups into the triazole ring that facilitates both hydrophobic and hydrogen-bond interaction with the surrounding amino acids of S′2 pocket, may improve ligand-enzyme interactions. The docking poses of the nine selected derivatives for synthesis are depicted in Fig. 1. (see the supplementary data Table S3 for all docked structure).

Overall, candidates were selected based on (i) H-bound interactions with the key catalytic residues of BACE1 active site (Asp32, Asp228), (ii) stacking interaction with the amino acids of the flap pocket, specially Tyr71 and/or Trp76 (iii) H-bound interactions with the Gly34 and/or Gly230 (iv) Occupation of a key pocket within the active site such as S2 and S′2 (v) and the lowest binding free energies (ΔG_b) in the desired orientation.

2.2. Chemistry

To evaluate the influence of aminomethylene triazole-containing iminochromene-2H-carboxamides on BACE1 activity and neuroprotection, the top 9 derivatives were synthesized. 1-Bromo-2-nitro-N-(prop-2-yn-1-yl)aniline was obtained following a nucleophile substitution of 4-dibromo-2-nitrobenzene with propagylamine (Scheme 3).

Various triazole derivatives were prepared by click reaction between the previously prepared molecule and the appropriate aromatic compound (Scheme 3). As it is depicted in Scheme 3d, reduction of nitro group of compounds **3a**–**i** was performed using aqueous solution of sodium carbonate and sodium dithionate in good yield. Cyanoacetylation of synthesized amines was done with the reaction of 2-cyanoacetyl-3,5-dimethyl pyrazole intermediate with **4a-i** (Scheme 4). To synthesize the final products, salicylaldehyde was reacted with 7a-i derivatives through Knoevenagel condensation (Scheme 4).

2.3. BACE1 enzymatic assay

The BACE1 inhibitory activity of each compound was tested at multiple concentrations and IC_{50} values were calculated (Table 1). The results of the *in vitro* BACE1 inhibition experiments were in agreement with the molecular docking and computational analysis. According to the obtained data, bromo-phenyl iminochromene-2H-carboxamide derivatives containing various aminomethylene triazole scaffolds demonstrated moderate to strong inhibitory potential against BACE1 enzyme at 10 and 50 μM concentrations.

a) Substitution of phthalimide on amino methylene triazole plays a significant role in BACE1 inhibition. Compound **8b** containing a phthalimide pendant on amino methylene triazole was the most potent derivative with IC_{50} value of 2.2 ± 0.5 μM. Elongation of the ethylene linker between the phthalimide group and triazole ring partially reduced the inhibitory potential of compound **8c** (IC_{50} = 6.8 ± 0.9 μM).
b) Based on the enzyme inhibition comparison of **8d** and **8e** with **8a**, it could be assumed that introduction of small lipophilic groups such as methoxy or methyl substitutes into the amino methylene triazole linker may not significantly alter the potency of compounds against BACE1.
c) Compound **8i** bearing 4-bromophenyl moiety inhibited BACE1 with an IC_{50} of 6.4 ± 2.4 μM and could be considered as another potent derivative against BACE1. Compound **8g** bearing a 3,4 di-chlorophenyl moiety demonstrated superior BACE1 inhibitory potential (IC_{50} = 7.5 ± 1.4 μM) over a 2,3 di-chlorophenyl containing counterpart (IC_{50} = 15.6 ± 7.4 μM). It suggests that the positioning of such electron withdrawing substituted groups might affect the ligand-BACE1 binding interaction.

In general, as depicted in Fig. 1 H-bound interaction of aminomethylene with Asp32 and amide linker with Asp228 were observed in most cases which confirm the BACE1 inhibitory of synthesize compounds. As depicted in Fig. 1-**8b**, two key residues of the binding site Asp32 and Asp228 are involved in hydrogen bond interactions with the amino methylene triazole linker and amide linker, respectively. The additional hydrogen bond interaction with Gly230 as a second important amino acid was observed through the amide linker. π-π stacking interaction was observed between Tyr71 and the bromophenyl ring. The phthalimide moiety establishes favorable π-π stacking interaction with side chain of Thr76.

2.4. Protection of neuronal PC12 cells exposed to Aβ25-35

The toxic effects of Aβ have been broadly examined. Recently, efforts have focused on designing new compounds in the hope to protect neural cells against the side effects of Aβ [24,25]. To our knowledge, there has been no research published on the neuroprotective properties of iminochromene derivatives. In order to

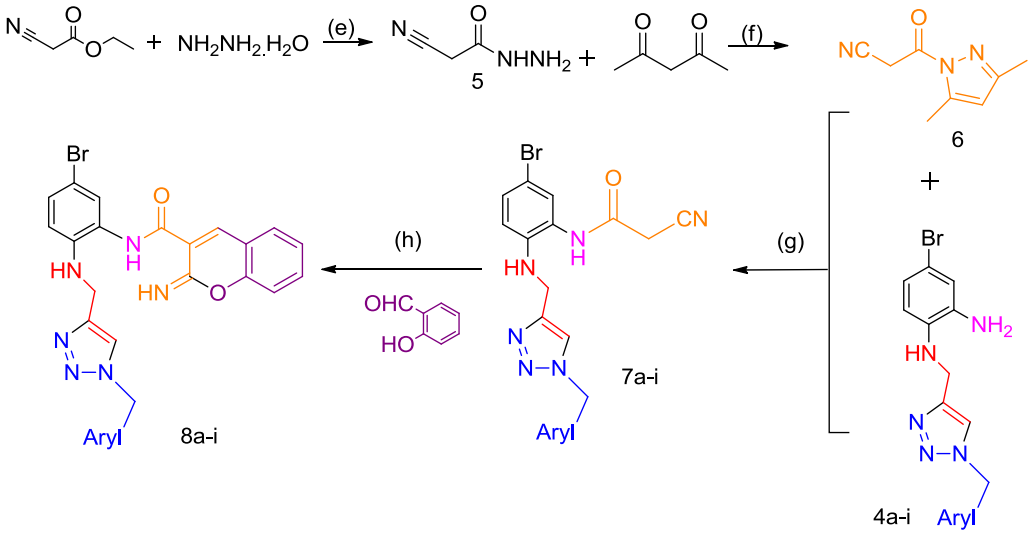

Scheme 4. Synthesis of imino-2H-chromen-3-carboxamide derivatives **8a-i.** (e) neat, rt; (f) water, 2 h, rt. (g) toluene, reflux (10 min), rt (overnight); (h) piperidine, MeOH, 50 °C, 7 h.

investigate the neuroprotective role of our synthesized compounds, PC12 cells were treated by these derivatives and then challenged with Aβ25−35. In the absence of any synthesized derivatives, the cells that were treated with Aβ showed 43.4 ± 2.2% viability compared to control untreated cells (Table 2). Caffeic acid as a positive control protected the PC12 cells with an IC_{50} value of 75.8 ± 11.3 μM. Significant protection was observed with compounds **8b** and **8c** containing phthalimide motifs with IC_{50} values of 7.9 μM and 6.8 μM, respectively. The percentage of protection of PC12 cells challenged with Aβ25−35 with 10 μM of compounds **8b** and **8c** were 78.8 and 67.8%, respectively. The cytotoxicity of synthesized derivatives against PC12 cells was also tested. The compounds did not show any cytotoxicity up to the concentration of 100 μM.

2.5. Metal chelating effect

Results of metal chelating assay of the most potent compounds are demonstrated in Table 3. Ferrozine forms a complex with ferrous ions and produces a magenta color. In the presence of chelating agents, formation of ferrous-ferrozine complex is blocked and as a result, absorbance is decreased. Compound **8i** showed acceptable biometal-chelating ability compared to EDTA as a well-known chelator [32].

2.6. Iron-chelating properties

The ability of **8i** to chelate Fe^{+2} as biometals was studied by UV-VIS spectroscopy using mole ratio method. In this method the total molar concentration of Fe(II) was continuously varied, while the molar concentration of the tested ligand was kept constant throughout the series of samples [33]. According to Fig. 2A the UV absorption of compound **8i** in methanol demonstrated three sharp picks in 353, 302 and 293 nm. As shown in Fig. 2A, the addition of Fe^{+2} to **8i** does not lead to a red or blue shift of wavelength but increased the maximum absorbance intensity initially at fix amount of **8i** and then plateaued. Fig. 2B indicates that under the experimental conditions the stoichiometry for the Fe^{+2}-**8i** complexes was 1.5, suggesting a complex with 3:2 [Fe^{+2}-**8i**] molar ratio.

2.7. Physicochemical parameters prediction

All the compounds were predicted by ADMET SAR to have moderate Blood-Brain Barrier (BBB) permeability (Table 4).

3. Conclusion

In conclusion, fragment based and hybrid design strategies were used to design a novel series of anti-Alzheimer agents with multiple modes of action including BACE1 inhibition, neuroprotection, and metal chelation. Considering the results of the present study, we conclude that bromo phenyl iminochromene-2H-carboxamides containing aminomethylene triazole pendants could be potentially useful scaffold for the discovery of anti-Alzheimer agents. Based on the BACE1 molecular docking, the amide and aminomethylene linkers of the designed compounds will maintain their critical roles of hydrogen bond interactions with the catalytic dyad in the most derivatives. Generally, the triazole pendant oriented toward the flap pocket and, this moiety was synthesized via a click reaction as a metal chelating fragment and developed via a diverse library of anti-Alzheimer agents. In addition, imino-2H-chromen of the designed scaffold would be indispensable for efficacy, solubility and BBB penetration of the scaffold.

Moreover, these derivatives showed significant neuroprotective activity. Among them, compound **8b** and **8c** had the highest level of neuronal protection which decreases IC_{50} to at least ten orders of magnitude in comparison with positive control. Most of the derivatives also showed interesting BACE1 inhibitory potency. Among the studied compounds, **8b** and **8c** demonstrated good inhibitory effect against BACE1. The affinity of some synthesized compounds for ferrous ions as nontoxic chelating ligands proposes them as potential agents for chelation therapy as well. The compounds **8b** and **8c** would provide a promising lead for further optimization in targeting Alzheimer's disease.

4. Material and method

4.1. Molecular docking

To select the best BACE1 inhibitor candidates for synthesis, a library of small molecules with various motifs at position Y and

Table 1
BACE1 inhibitory activity of test compounds (**8a-i**) assessed by BACE1-FRET assay.

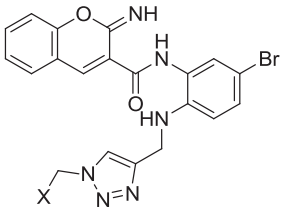

Compounds	Structure	IC_{50}[a]	% Inhibition at 50 μM[a/b]	% Inhibition at 10 μM[a/b]
8a		–	25.2 (±0.1)	12.1 (±0.4)
8b	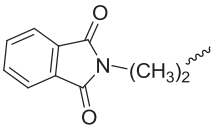	2.2 (±0.5) (μM)	84.2 (±2.1)	83.5 (±2.3)
8c	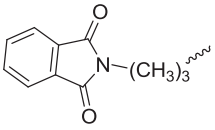	6.8 (±0.9) (μM)	77.6 (±5.9)	55.7 (±3.3)
8d	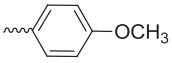	–	34.5 (±5.5)	10.0 (±0.3)
8e	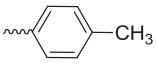	–	52.4 (±3.3)	38.3 (±4.2)
8f	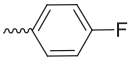	–	45.9 (±6.3)	21.3 (±4.8)
8g	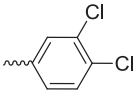	7.5 (±1.4) (μM)	60.8 (±2.0)	52.0 (±3.4)
8h	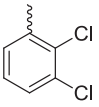	15.6 (±7.4) (μM)	62.0 (±4.6)	47.8 (±3.4)
8i	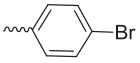	6.4 (±2.4) (μM)	100.0 (±7.2)	72.3 (±18.3)
OM99-2[c]		14.7 (±2.8) (nM)		

[a] Presented data are the mean (±S.E.M.) of three to five independent determinations.
[b] % Inhibition were calculated at four different concentrations (50, 10, 1 and 0.1 μM). However, just 50 and 10 μM were reported.
[c] OM99-2 was used as a positive control.

then X were drawn using HyperChem and energetically minimized with MM^+ force field. The Gastiger charges and torsional degrees of freedom were assigned to the generated PDB files. The X-ray crystallographic structures were retrieved from the Brookhaven protein data bank (http://www.rcsb.org/). Virtual screening of designed library was done using Autodock 4.2 and Auto Dock Tools 1.5.4 (ADT). Water molecules and the cognate ligand were removed from the receptor. All hydrogens were properly added to the receptor PDB and non-polar hydrogens were merged into related atoms of the receptor using ADT. Kollman charges were also assigned. The grid maps were calculated with AutoGrid (part of the AutoDock package). The created three-dimensional grids were 60*60*60 (x, y, z) with a grid spacing of 0.375 Å and the cubic grids were centered on the binding site of native ligand. Lamarckian genetic algorithm (LGA) was applied to model the interaction/binding between the ligand and the BACE1 active site. For Lamarckian GA, 27,000 maximum generations, a gene mutation rate of 0.02, population size of 100 and a cross over rate of 0.8 were used [34]. Scoring function of AD 4.2 includes five energy terms: van der Waals term, hydrogen binding term, electrostatic term, desolvation term and the term for loss of torsional entropy of ligand upon binding. In the actual docking simulation of a compound in the docking library, the empirical scoring function of the original Auto Dock program was employed [35].

4.1.1. Selection of pdb code

In order to find a suitable x-ray crystallographic structure of BACE1 for virtual study, thirteen pdb structures were chosen based on the similarity of their cognate ligands with our designed structure. Among the 13 different pdb structures, 1w51 was selected because of its optimal self-docking results (free energies of −9.5 kcal/mol, RMSD 0.6, resolution 1.7 Å and number in cluster)

Table 2
Inhibition of Aβ induced neurotoxicity in PC12 neuronal cells by synthesized derivatives.

Compounds	IC_{50} (μM)[a]	% Protection at 25 μM[a]	% Protection at 10 μM[a]
8a	–	ND	ND
8b	7.9 (±1.7)	100	78.8 (±18.1)
8c	6.8 (±1.0)	ND[b]	67.8 (±10.4)
8d	–	22.0 (±0.4)	28.4 (±2.4)
8e	–	19.2 (±9.1)	ND
8f	–	22.2 (±9.9)	13.1 (±9.9)
8g	90.5 (±32.2)	49.8 (±12.6)	21. 8 (±7.3)
8h	18.9 (±4. 9)	57.2 (±14.5)	23.6 (±10.5)
8i	37.8 (±9.2)	37.5 (±6.9)	16.4 (±7.3)
Caffeic acid[c]	75.8 (±11.3)	–	–

[a] Protection against Aβ-induced PC12 cell death was measured with MTT assay. The data are expressed as the mean (±S.E.M.) of three to five independent experiments.
[b] The % protection was not measured at 25 μM, but it was 83. 8 ± 7. 7 μM at 15 μM.
[c] Caffeic acid was used as a positive control.

Table 3
Metal chelating activity of synthesized compounds determined by a colorimetric method.

Code	Percent of Fe^{2+} chelating at 400 μmol/L[a]
8b	10.2 ± 1.3
8c	12.8 ± 1.4
8i	45.2 ± 2.1
EDTA[b]	96.4 ± 5.3

[a] Values represent the mean of three independent experiments ± S.E.M.
[b] EDTA was used as a positive control.

The results of self-docking are summarized in Table S4.

4.2. Chemistry

All the reagents were purchased from commercial sources and used without further purification. ^1H and ^{13}C NMR spectra were determined by a Bruker FT-300 MHz spectrometer in $CDCl_3$ or DMSO-d_6. All the chemical shifts were reported as (δ) values (ppm) against tetra methyl silane as an internal standard. CHNOS analysis was performed using the ECS4010 from Costech Company. The MS spectra were recorded using Agilent 7000-3Q mass spectrometer at an electron impact mode with an ionization voltage of 70 eV. The IR spectra were obtained on a FT-IR Perkin–Elmer Precisely system spectrophotometer (potassium bromide disks). Melting points were determined on a Kofler hot stage apparatus and are uncorrected. Merck silica gel 60 F254 plates were used for analytical TLC. Preparative thin-layer chromatography was done with prepared glass-backed plates (20*20 cm^2, 500 μ) using silica gel (MerkKieselgel60 HF254, Art. 7739). Preparative column chromatography was carried out on silica gel (230–400 mesh, G60 Merck).

4.2.1. General procedures

*4.2.1.1. Synthesis of 4-bromo-2-nitro-N-(prop-2-yn-1-yl)aniline (**1**).* The alkyne derivative **1** was synthesized in DMF under reflux condition for 24 h by the reaction of 1,4-dibromo-2-nitrobenzene (10 mmol) with propagylamine (20 mmol) in presence of a catalytic amount of triethylamine. The product was purified by flash chromatography on silica gel, using 10% ethyl acetate in petroleum ether as the eluent, affording the product as an orange powder. Yield 54%; MP: 80–84 °C; MS: *m/z*(%) 256 ($(M+2)^+$, 41), 254 (M^+, 41), 209 (40), 207 (40), 185 (45), 183 (100), 181 (62), 171 (22), 169 (22), 129 (45), 128 (62), 102 (68), 90 (22), 75 (30), 63 (37); ^1H NMR ($CDCl_3$, 300 MHz): δ_H (ppm) = 2.24 (s, 1H, alkyn-H), 4.04–4.06 (dd, 2H, *J* = 3, 5.7 Hz, CH_2), 6.81–6.84 (d, 2H, *J* = 9.0 Hz, Ar-H), 7.48–7.52 (dd, 1H, *J* = 2.4, 9 Hz, Ar-H), 8. 033 (s, 1H, NH), 8.263–8.271 (d, 1H, *J* = 2.4 Hz, Ar-H).

*4.2.1.2. Synthesis of aryl substituted derivatives of 4-bromo-N-((1-methyl-1H-1,2,3-triazol-4-yl)methyl)-2-nitroaniline (**3a-i**).* Different derivatives of intermediates **2a-i** were prepared in situ via reaction of the appropriate alkyl or halide (7 mmol) with sodium azide (7 mmol) in the presence of triethylamine in *t*-BuOH/water. After around 30 min, 4-bromo-2-nitro-N-(prop-2-yn-1-yl)aniline (6.5 mmol), $CuSO_4 \cdot 5H_2O$ (10 mol%) and sodium ascorbate (25 mol %) were added to 2a-i. [36,37]. The mixture was stirred at room temperature for 48 h and an orange precipitate was produced. Produced solids were washed with water several times. Further purification was performed using column chromatography with a decreasing ratio of petroleum ether to ethyl acetate (90:10 to 50:50) to produce the desired products **3a-i**.

*4.2.1.3. N-((1-benzyl-1H-1,2,3-triazol-4-yl)methyl)-4-bromo-2-nitroaniline (**3a**).* Benzyl bromide (7 mmol) and NaN_3 (6.9 mmol) in the presence of triethylamine in *t*-BuOH/water was stirred in room temperature for 30 min and then 4-bromo-2-nitro-N-(prop-2-yn-1-yl)aniline **1**, $CuSO_4 \cdot 5H_2O$ (10 mol%) and sodium ascorbate (25 mol%) were added. The mixture was stirred at room temperature for 48 h and an orange participate was produced. The resulted precipitate was filtered off, washed with water and diethyl ether and recrystallized from ethanol. Yield 62%; MP: 189–191 °C; MS: *m/z* (%) 389 ($(M+2)^+$, 5), 387 (M^+, 5), 343 (18), 341 (18), 104 (8), 91 (100), 77 (6), 65 (14); ^1H NMR (DMSO-d_6, 300 MHz): δ_H (ppm) = 4.69 (s, 2H, CH_2), 5.57 (s, 2H, CH_2), 7.07–7.10 (d, 1H, *J* = 9.3 Hz, Ar-H), 7.29–7.36 (m, 5H, Ar-H), 7.60–7.63 (dd, 1H, *J* = 2.1, 9.3 Hz, Ar-H), 7.85 (s, 1H, Ar-H), 8.16–8.17 (d, 2H, *J* = 2.1 Hz, Ar-H).

*4.2.1.4. Synthesis of aryl substituted derivatives of 4-bromo-N1-((1-methyl-1H-1,2,3-triazol-4-yl)methyl)benzene-1,2-diamine (**4a-i**).* The nitro compound **3a–i** (6.7 mmol) was dissolved in methanol (25 ml). The metabolic solution of nitro compound was added drop wise (using dropping funnel) to an aqueous solution of sodium carbonate (6.5 g, 61.3 mmol) and sodium dithionite (13 g, 74.4 mmol) containing 100 ml water at 70 °C. When all of the nitro starting material was added to mixture, the mixture was stirred at 70 °C for 2 h to complete the reaction (Checked by TLC). To remove methanol of mixture, it was evaporated under reduced pressure and the resultant aqueous mixture was extracted with ethyl acetate, and dried with Na_2SO_4, filtered, and concentrated. The resulting product was further purified using preparative thin layer chromatography chloroform/EtOH (90:10).

*4.2.1.5. N1-((1-benzyl-1H-1,2,3-triazol-4-yl)methyl)-4-bromobenzene-1,2-diamine (**4a**).* Brown oily product; Yield 87%; MS: *m/z* (%) 359 ($(M+2)^+$, 80), 357 (M^+, 80), 187 (33), 144 (40), 118 (10), 91 (100), 65 (15); ^1H NMR ($CDCl_3$, 300 MHz): δ_H (ppm) = 3.41 (brs, 2H, NH_2), 4.23 (s, 2H, CH_2), 5.35 (s, 2H, CH_2), 6.36–6.39 (d, 1H, *J* = 6.0 Hz, Ar-H), 6.67–6.73 (m, 2H, Ar-H), 7.11–7.13 (brm, 2H, Ar-H), 7.245 (s, 6H, Ar-H).

*4.2.1.6. Synthesis of 3-(3,5-dimethyl-1H-pyrazol-1-yl)-3-oxopropanenitrile (**6**).* 2-cyano acetohydrazide (compound **5**) was synthesized by the reaction of hydrazine hydrate and ethyl 2-cyanoacetate as previously described (yield: 97%) [38]. An equimolar amount of compound 5 was reacted with acetyl acetone in the presence of a catalytic amount of HCl in water (15 ml). The mixture was stirred at room temperature for 2 h. The white precipitate (Scheme 4, compound **6**) was filtered off, washed with cold

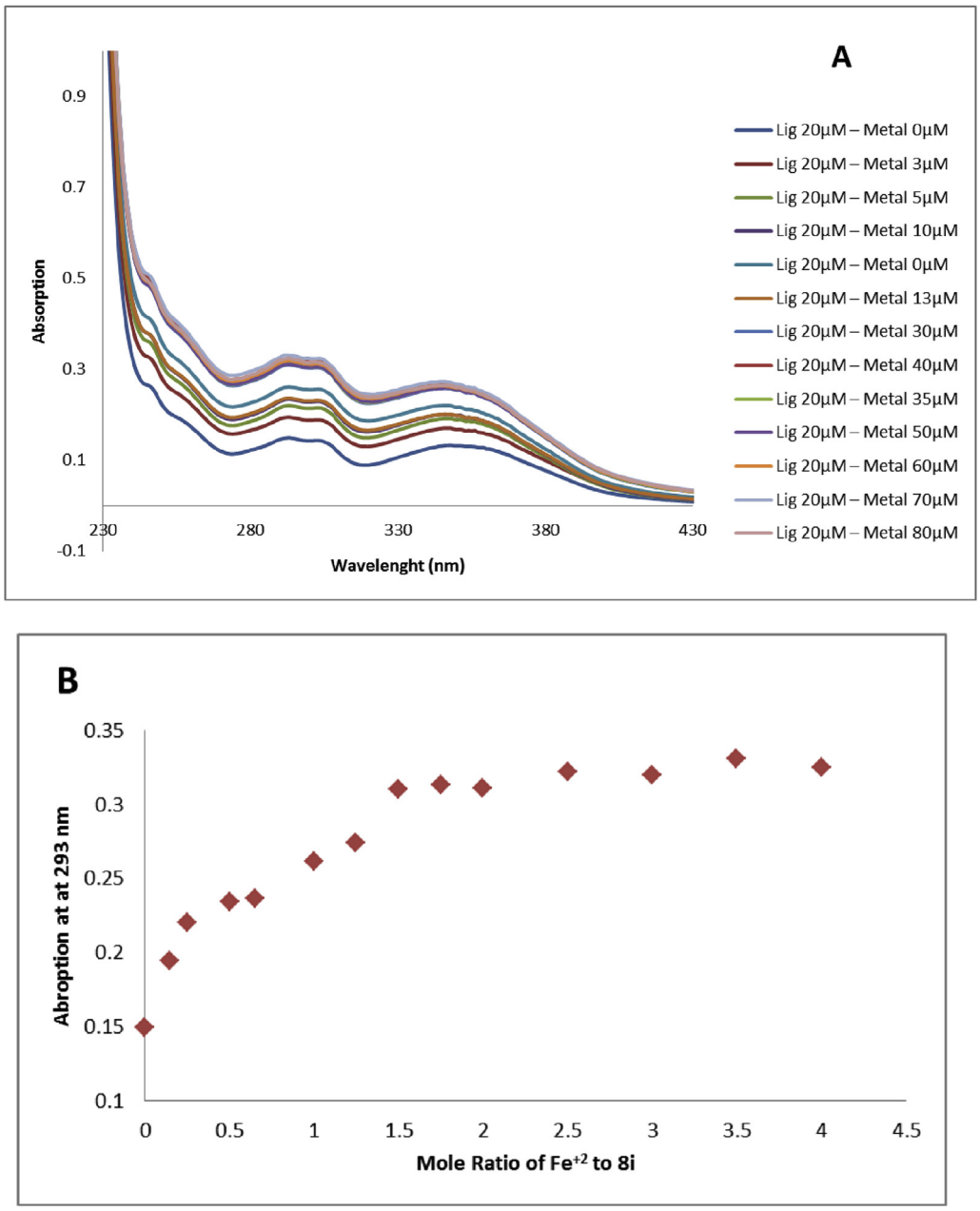

Fig. 2. (A) UV spectrum of compound **8i** (final concentration was 20 μM) alone or in the presence of Fe(II) (the final concentration of Fe^{+2} ranged from 0 μM to 80 μM). (B) Determination of the stoichiometry of complex Fe^{+2}-8i using molar ratio method through titrating the methanol solution of compound **8i** with ascending amounts of Fe(II).

Table 4
Summary of physicochemical properties of synthesized compounds.

Compound	BBB penetration[a]		H- bond donor[b]	H- bond acceptor[b]	Molar Refractivity[b]
	%	CNS activity			
8a	0.9	+	4	7	129.6
8b	0.5	+	5	11	147.5
8c	0.5	+	4	10	147.7
8d	0.6	+	4	8	134.4
8e	0.8	+	5	8	136.2
8f	0.9	+	4	7	128.9
8g	0.9	+	4	7	137.2
8h	0.9	+	4	7	142.1
8i	0.9	+	4	7	129.1

[a] http://lmmd.ecust.edu.cn:8000/predict/.
[b] http://www.scfbio-iitd.res.in/software/drugdesign/lipinski.jsp.

water and subsequently dried in an oven. Yield 91%; MS: *m/z* (%) 163 (M^+, 46), 135 (23), 121 (8), 95 (100), 81 (11.5), 68 (10), 54 (5), 39 (12); ^{1}H NMR ($CDCl_3$, 400 MHz) δ_H (ppm): 2.23 (s, 3H, $C\underline{H}_3$), 2.55 (s, 3H, $C\underline{H}_3$), 4.29 (s, 2H, $C\underline{H}_2$-CN), 6.03 (s, 1H, Pyrazole-$\underline{H}$).

*4.2.1.7. Synthesis of aryl substitiated derivatives of N-(5-bromo-2-(((1-methyl-1H-1,2,3-triazol-4-yl)methyl)amino)phenyl)-2-cyanoacetamide (**7a-i**).* The 3-(3,5-dimethyl-1H-pyrazol-1-yl)-3-oxopropanenitrile **6** (1.2 g, 7 mmol) was added to a solution of different aryl substituted derivatives of 4-bromo-N1-((1-methyl-1H-1,2,3-triazol-4-yl)methyl)benzene-1,2-diamine **4a-i** in toluene (10 ml). The mixture was refluxed for 30 min and then stirred at room temperature overnight. The resulting precipitate was filtered off, washed with Et_2O and further purified by thin layer chromatography using chloroform/EtOH (97:3) to afford compound **7a–i** as pure solid product.

*4.2.1.8. Synthesis of N-(2-(((1-benzyl-1H-1,2,3-triazol-4-yl)methyl) amino)-5-bromophenyl)-2 cyanoacetamide (**7a**).* Brown powder; Yield 51%; MS: *m/z* (%) 426 ($(M+2)^+$, 7), 424 (M^+, 7), 408 (20), 406 (20), 383 (7), 144 (13), 115 (6), 104 (6), 91 (100); ^{1}H NMR ($CDCl_3$, 300 MHz) δ_H (ppm) = 4.25 (s, 2H, $C\underline{H}_2$), 5.35 (s, 2H, $C\underline{H}_2$), 5.38 (s, 2H, $C\underline{H}_2$), 7.03–7.05 (d, 1H, J = 7.5 Hz, Ar-$\underline{H}$), 7.29–7.33 (m, 2H, Ar-$\underline{H}$), 7.41–7.43 (m, 4H, Ar-$\underline{H}$), 7.48–7.52 (m, 1H, Ar-$\underline{H}$), 7.8103 (s, 1H, Ar-$\underline{H}$).

*4.2.1.9. Synthesis of different derivatives of N-(5-bromo-2-(((1-methyl-1H-1,2,3-triazol-4-yl)methyl)amino)phenyl)-2-imino-2H-chromene-3-carboxamide (**8a-i**).* An equimolar mixture of salicylaldehyde (5 mmol), aryl substituted analogues of N-(5-bromo-2-(((1-methyl-1H-1,2,3-triazol-4-yl)methyl)amino)phenyl)-2-cyanoacetamide (**7a-i**) (5 mmol), methanol (10 ml) and a catalytic amount of piperdine (0.1 ml) was stirred at 50 °C for 6–7 h. After cooling, the yellow precipitate was filtered, washed with Et_2O and subsequently dried under reduced pressure. The resulting residue was further purified using thin layer chromatography using chloroform/EtOH (85:15) to afford yellow precipitate.

*4.2.1.10. Synthesis of N-(2-(((1-benzyl-1H-1,2,3-triazol-4-yl)methyl) amino)-5-bromophenyl)-2-imino-2H-chromene-3-carboxamide (**8a**).* Pale yellow powder; MP 210–216 °C; Yield 76%; IR ($CDCl_3$, cm^{-1}) ν_{max} = 3683 (NH), 3620 (NH), 3584 (NH), 3019 (CH), 1710 (C=O; C=N), 1260 (C-N), 1216 (C-O); MS: *m/z* (%) 532 ($(M+2)^+$, 1.5), 530 (M^+, 1.5), 515 (25), 513(25), 394 (45), 392 (45), 367 (10), 342 (23), 340 (23), 312 (15), 314 (15), 212 (21), 144 (17), 120 (23), 106 (40), 91 (100), 77 (21); ^{1}H NMR (DMSO-d_6, 300 MHz) δ_H (ppm): 5.66 (s, 2H, $C\underline{H}_2$), 5.92 (s, 2H, $C\underline{H}_2$), 7.14–7.16 (d, 1H, J = 8.7 Hz, Ar-$\underline{H}$), 7.32–7.42 (m, 7H, Ar-$\underline{H}$), 7.58–7.64 (m, 1H, Ar-$\underline{H}$), 7.70–7.77 (m, 2H, Ar-$\underline{H}$), 7.84–7.87 (d, 1H, J = 8.7 Hz, Ar-$\underline{H}$), 8.33–8.38 (m, 3H, Ar-$\underline{H}$), 9.093 (s, 1H, C$\underline{H}$ (iminochromene)); ^{13}C NMR (DMSO-d_6,75 MHz) δ_C (ppm): 51.4, 78.1, 108.1, 114.2, 115.8, 118.9, 120.0, 120.5, 121.4, 123.0, 124.3, 125.7, 126.9, 128.1, 130.2, 131.7, 133.3, 135.7, 138.5, 140.1, 141.4, 145.7, 149.3, 153.7, 156.3, 160.4; $C_{27}H_{23}BrN_6O_3$: C 57.97, H 4.14, N 15.02. Found: C 57.92, H 4.14, N 15. 00; $C_{26}H_{21}BrN_6O_2$: C 58.99, H 4.00, N 15.87. Found: C 58.93, H 4.05, N 15. 90.

*4.2.1.11. Synthesis of N-(5-bromo-2-(((1-(2-(1,3-dioxoisoindolin-2-yl)ethyl)-1H-1,2,3-triazol-4-yl)methyl) amino) phenyl)-2-imino-2H-chromene-3-carboxamide (**8b**).* Yellow powder; Yield 86%; MP 238–242 °C; IR ($CDCl_3$, cm^{-1}) ν_{max} = 3690 (NH), 3650 (NH), 3615 (NH), 3019 (CH), 1710 (C=O; C=N), 1261 (C-N), 1216 (C-O); MS: *m/z* (%) 613($(M+2)^+$, 0.5), 611 (M^+, 0.5), 598 (20), 596 (20), 411 (22), 409 (22), 394 (100), 392 (100), 342 (30), 340 (30), 314 (16.5), 174 (28), 160 (40), 146 (24), 104 (10); ^{1}H NMR (DMSO-d_6, 300 MHz) δ_H (ppm): 3.73–3.75 (t, 2H, J = 6.0 Hz, $C\underline{H}_2$), 4.00–4.02 (t, 2H, J = 6.0, $C\underline{H}_2$), 5.59 (s, 2H, $C\underline{H}_2$), 6.73–6.76 (d, 1H, J = 7.4 Hz, Ar-$\underline{H}$), 7.23–7.30 (m, 4H, Ar-$\underline{H}$), 7.55–7.58 (m, 3H, Ar-$\underline{H}$), 7.89–8.01 (m, 5H, Ar-$\underline{H}$), 8.53 (s, 1H, N$\underline{H}$ (iminochromene)), 9.20 (s, 1H, C$\underline{H}$ (iminochromene)), 12.26 (s, 1H, N$\underline{H}$CO); ^{13}C NMR (DMSO-d_6,75 MHz) δ_C (ppm): 52.43, 55.21, 81.19, 107.06, 109.81, 112.48, 114.22, 115.59, 117.2, 120.8, 122.2, 123.7, 126.8, 128.8, 129.5, 130.6, 132.1, 133.7, 135.1, 138.4, 140.6, 141.7, 143.3, 146.9, 149.9, 152.3, 154.6, 156.3, 161.2; $C_{29}H_{22}BrN_7O_4$: C 56.87, H 3.62, N 16.01. Found: C 56.92, H 3.60, N 15. 94.

*4.2.1.12. Synthesis of N-(5-bromo-2-(((1-(3-(1,3-dioxoisoindolin-2-yl)propyl)-1H-1,2,3-triazol-4-yl)methyl) amino) phenyl) -2-imino-2H-chromene-3-carboxamide (**8c**).* Yellow powder; Yield 84%; MP 230–235 °C; IR ($CDCl_3$, cm^{-1}) ν_{max} = 3684 (NH), 3610 (NH), 3584 (NH), 3019 (CH), 1710 (C=O; C=N), 1261 (C-N), 1216 (C-O); MS: *m/z* (%) 627 ($(M+2)^+$, 0.1), 625 (M^+, 0.1), 530 (50), 359 (36), 357 (36), 339 (40), 337 (40), 324 (27.4), 322 (28), 316 (20), 314 (20),172 (100), 145 (70), 118 (60), 89 (50); ^{1}H NMR (DMSO-d_6, 300 MHz) δ_H (ppm): 2.145 (brm, 2H, $C\underline{H}_2$), 3.56 (brm, 2H, $C\underline{H}_2$), 3.70 (brm, 2H, $C\underline{H}_2$), 5.58 (s, 2H, $C\underline{H}_2$), 6.73–6.75 (d, 1H, J = 7.0 Hz, Ar-$\underline{H}$), 7.23–7.29 (m, 4H, Ar-$\underline{H}$), 7.55–7.58 (m, 3H, Ar-$\underline{H}$), 7.84 (s, 4H, Ar-$\underline{H}$), 7.99 (s, 1H, Ar-$\underline{H}$), 8.52 (s, 1H, N$\underline{H}$ (iminochromene)), 9.19 (s, 1H, C$\underline{H}$ (iminochromene)), 12.27 (s, 1H, N$\underline{H}$CO); ^{13}C NMR (DMSO-d_6, 75 MHz) δ_C (ppm): 32.3, 52.4, 52.8, 80.9, 108.2, 110.3, 114.5, 115.4, 118.9, 121.0, 123.4, 124.7, 126.2, 126.9, 128.5, 130.5, 132.0, 133.7, 134.7, 136.1, 138.4, 140.7, 141.7, 146.2, 150.5, 153.9, 156.1, 160.7, 163.7, 165.6; $C_{30}H_{24}BrN_7O_4$: C 57.52, H 3.86, N 15.65. Found: C 57.49, H 3.89, N 15. 67.

*4.2.1.13. Synthesis of N-(5-bromo-2-(((1-(4-methoxybenzyl)-1H-1,2,3-triazol-4-yl)methyl)amino)phenyl)-2-imino-2H-chromene-3-carboxamide (**8d**).* Yellow powder; Yield 84%; MP 234–237 °C; IR ($CDCl_3$, cm^{-1}) ν_{max} = 3670 (NH), 3583 (NH), 3401 (NH), 3018 (CH), 1622 (C=O; C=N), 1218 (C-N), 1216 (C-O),1053 (C-O); MS: *m/z* (%) 544 ($(M+2)^+$, 0.7), 542 (M^+, 0.7), 427 (32), 392 (30), 342 (30), 340 (30), 323 (21), 321 (21), 211 (17), 121 (100), 91 (35), 77 (22), 63 (16); ^{1}H NMR (DMSO-d_6, 300 MHz) δ_H (ppm): 3.72 (s, 3H, $C\underline{H}_3$), 5.40 (s, 2H, $C\underline{H}_2$), 5.55 (s, 2H, $C\underline{H}_2$), 6.83–6.86 (d, 2H, J = 8.4 Hz, Ar-$\underline{H}$), 7.14–7.16 (d, 2H, J = 8.4 Hz, Ar-$\underline{H}$), 7.44–7.56 (m, 4H, Ar-$\underline{H}$), 7.68–7.77 (m, 3H, Ar-$\underline{H}$), 7.85–7.90 (m, 2H, Ar-$\underline{H}$), 8.00 (s, 1H, N$\underline{H}$ (iminochromene)), 8.51 (s, 1H, C$\underline{H}$ (iminochromene)); ^{13}C NMR (DMSO-d_6,75 MHz) δ_C (ppm): 59.3, 76.0, 80.7, 108.3, 112.9, 116.8, 122.2, 122.5, 123.4, 123.6, 125.2, 127.4, 128.5, 130.4, 130.8, 130.9, 134.1, 134.4, 140.0, 145.0, 149.1, 152.3, 154.5, 158.4, 159.1, 161.8, 167.3; $C_{27}H_{23}BrN_6O_3$: C 57.97, H 4.14, N 15.02. Found: C 57.92, H 4.14, N 15. 00.

*4.2.1.14. Synthesis of N-(5-bromo-2-(((1-(4-methylbenzyl)-1H-1,2,3-triazol-4-yl)methyl)amino)phenyl)-2-imino-2H-chromene-3-carboxamide (**8e**).* Yellow powder; Yield 81%; MP 215–219 °C; IR ($CDCl_3$, cm^{-1}) ν_{max} = 3671 (NH), 3584 (NH), 3404 (NH), 3020 (CH), 1710 (C=O; C=N), 1363 (C-N), 1216 (C-O); MS: *m/z* (%) 543 ($(M+2)^+$, 2), 541 (M^+, 2), 527 (10), 525 (10), 394 (100), 394 (100) 342 (36), 340 (36), 314 (14), 312 (14), 143 (14), 105 (57), 91 (50), 77 (15); ^{1}H NMR (DMSO-d_6, 300 MHz) δ_H (ppm): 1.23 (s, 3H, $C\underline{H}_3$), 4.38 (s, 2H, $C\underline{H}_2$), 5.57 (s, 2H, $C\underline{H}_2$), 6.73–6.76 (d, 1H, J = 8.1 Hz, Ar-$\underline{H}$), 7.08–7.17 (m, 3H, Ar-$\underline{H}$), 7.20–7.24 (m, 4H, Ar-$\underline{H}$), 7.31–7.33 (m, 2H, Ar-$\underline{H}$), 7.35–7.56 (d, 1H, J = 8.1, Ar-$\underline{H}$), 7.72–7.74 (d, 1H, J = 7.2 Hz, Ar-$\underline{H}$), 7.90 (s, 1H, Ar-$\underline{H}$), 8.03 (s, 1H, N$\underline{H}$ (iminochromene)), 8.30 (s, 1H, C$\underline{H}$ (iminochromene)); ^{13}C NMR (DMSO-d_6,75 MHz) δ_C (ppm): 31.0, 52.4, 79.5, 105.5, 113.5, 115.9, 116.1, 116.2, 119.5, 123.1, 124.6, 124.8, 125.5, 130.0, 130.6, 131.5, 131.8, 132.7, 132.8133.0, 133.4, 143.6, 146.6, 153.6, 154.1, 159.8, 160.6; $C_{27}H_{23}BrN_6O_2$: C 59.68, H 4.27, N 15.47. Found: C 59.61, H 4.34, N 15. 53.

*4.2.1.15. Synthesis of N-(5-bromo-2-(((1-(4-fluorobenzyl) -1H-1,2,3-triazol-4-yl)methyl)amino)phenyl)-2-imino-2H-chromene-3-carboxamide (**8f**).* Yellow powder; Yield 83%; MP 235–240 °C; IR ($CDCl_3$, cm^{-1}) ν_{max} = 3683 (NH), 3585 (NH), 3406 (NH), 3020 (CH), 1710 (C=O; C=N), 1363 (C-N), 1216 (C-O); MS: *m/z* (%) 548 ($(M+2)^+$, 4), 546 (M^+, 4), 401 (6), 387 (15), 385 (15), 342 (11), 340 (11), 292 (9), 290 (9), 171 (29), 143(31), 109 (100), 77 (10); ^1H NMR (DMSO-d_6, 300 MHz) δ_H (ppm): 4.383 (s, 2H, C<u>H</u>$_2$), 5.57 (s, 2H, C<u>H</u>$_2$), 6.73–6.76 (d, 1H, *J* = 7.8 Hz, Ar-<u>H</u>), 7.08–7.18 (m, 2H, Ar-<u>H</u>), 7.21 (s, 1H, Ar-<u>H</u>), 7.22–7.25 (m, 4H, Ar-<u>H</u>), 7.31–7.34 (m, 2H, Ar-<u>H</u>), 7.51–7.56 (m, 1H, Ar-<u>H</u>), 7.30–7.75 (s, 1H, Ar-<u>H</u>), 7.90 (s, 1H, Ar-<u>H</u>), 8.04 (s, 1H, N<u>H</u> (iminochromene)), 8.313 (s, 1H, C<u>H</u> (iminochromene)). $C_{26}H_{20}BrFN_6O_2$: C 57.05, H 3.68, N 15.35. Found: C 56.99, H 3.71, N 15. 35.

*4.2.1.16. Synthesis of N-(5-bromo-2-(((1-(3,4-dichlorobenzyl)-1H-1,2,3-triazol-4-yl)methyl)amino) phenyl)-2-imino-2H-chromene-3-carboxamide (**8g**).* Yellow powder; Yield 72%; MP 227–230 °C; IR ($CDCl_3$, cm^{-1}) ν_{max} = 3681 (NH), 3584 (NH), 3407 (NH), 3020 (CH), 1710 (C=O; C=N), 1363 (C-N), 1216 (C-O); MS: *m/z* (%) 601 ($(M+4)^+$, 0.5), 599 ($(M+2)^+$ 1), 597 (M^+, 0.5), 581 (8), 579 (5.2), 502 (2.7), 500 (6.7), 498 (4.1), 392 (100), 390 (100), 342 (40), 340 (40), 314 (13), 312 (13), 290 (8), 288 (8), 159 (50), 143 (17), 115 (12), 89 (23), 63 (14); ^1H NMR (DMSO, 300 MHz) δ_H (ppm): 4.39 (s, 2H, C<u>H</u>$_2$), 5.54 (s, 2H, C<u>H</u>$_2$), 6.66–6.70 (d, 1H, *J* = 13.0 Hz, Ar-<u>H</u>), 7.01–7.14 (m, 5H, Ar-<u>H</u>), 7.30–7.37 (m, 5H, Ar-<u>H</u>), 7.77–7.82 (m, 2H, Ar-<u>H</u>), 8.81 (s, 1H, C<u>H</u> (iminochromene)); $C_{26}H_{19}BrCl_2N_6O_2$: C 52.20, H 3.20, N 14.05. Found: C 52.16, H 3.23, N 14. 06.

*4.2.1.17. Synthesis of N-(5-bromo-2-(((1-(2,3-dichlorobenzyl)-1H-1,2,3-triazol-4-yl)methyl)amino)phenyl)-2-imino-2H-chromene-3-carboxamide (**8h**).* Yellow powder; Yield 73%; MP 229–232 °C; IR ($CDCl_3$, cm^{-1}) ν_{max} = 3683 (NH), 3586 (NH), 3406 (NH), 3020 (CH), 1710 (C=O; C=N), 1362 (C-N), 1216 (C-O); MS: *m/z* (%) 601 ($(M+4)^+$, 1), 599 ($(M+2)^+$ 2), 597 (M^+, 1), 581 (10), 392 (100), 390 (100), 342 (50), 340 (50), 314 (20), 312 (20), 290 (18), 288 (18), 173 (40), 159 (80), 143 (27), 89 (32), 63 (24); ^1H NMR (DMSO-d_6, 300 MHz) δ_H (ppm): 4.41 (s, 2H, C<u>H</u>$_2$), 5.56 (s, 2H, C<u>H</u>$_2$), 6.67–6.71 (d, 1H, *J* = 12.0 Hz, Ar-<u>H</u>), 7.03–7.19 (m, 5H, Ar-<u>H</u>), 7.32–7.41 (m, 5H, Ar-<u>H</u>), 7.81–7.86 (t, 2H, *J* = 8.0 Hz, Ar-<u>H</u>), 8.44 (s, 1H, C<u>H</u> (iminochromene)); ^{13}C NMR (DMSO-d_6,75 MHz) δ_C (ppm): 57.3, 80.9, 109.6, 112.9, 115.2, 117.1, 117.4, 123.2, 123.3, 124.5, 125.5, 127.6, 128.8, 129.4, 131.6, 132.7, 134.2, 136.3, 143.2, 148.6, 152.5, 155.7, 158.8, 159.1, 162.5, 165.2; $C_{26}H_{19}BrCl_2N_6O_2$: C 52.20, H 3.20, N 14.05. Found: C 52.15, H 3.25, N 13. 98.

*4.2.1.18. Synthesis of N-(5-bromo-2-(((1-(4-bromobenzyl)-1H-1,2,3-triazol-4-yl)methyl)amino)phenyl)-2-imino-2H-chromene-3-carboxamide (**8i**).* Yellow powder; Yield 91%; MP 241–243 °C; IR ($CDCl_3$, cm^{-1}) ν_{max} = 3684 (NH), 3620 (NH), 3527 (NH), 3019 (CH), 1710 (C=O; C=N), 1452 (C-N), 1216 (C-O); MS: *m/z* (%) 610 ($(M+4)^+$, 0.3), 608 ($(M+2)^+$ 0.7), 606 (M^+, 0.3), 541 (11), 539 (12), 537 (12), 512 (13), 510 (27), 508 (14), 463 (28), 447 (26), 396 (16), 392 (16), 342 (51), 340 (51), 290 (44), 288 (44), 249 (20), 171 (100), 143 (46), 115 (19), 90 (38); ^1H NMR ($CDCl_3$, 300 MHz) δ_H (ppm): 4.43 (s, 2H, C<u>H</u>$_2$), 5.38 (s, 2H, C<u>H</u>$_2$), 6.51–6.54 (d, 1H, *J* = 8.4 Hz, Ar-<u>H</u>), 7.03–7.20 (m, 5H, Ar-<u>H</u>), 7.38–7.47 (m, 7H, Ar-<u>H</u>), 7.76 (s, 1H, NH (iminochromene)), 8.44 (s, 1H, C<u>H</u> (iminochromene)), 12.09 (s, 1H, N<u>H</u>CO); ^{13}C NMR (DMSO-d_6,75 MHz) δ_C (ppm): 52.4, 80.7, 108.3, 114.5, 115.4, 118.9, 119.4, 120.9, 121.7, 123.4, 124.7, 126.1, 126.7, 128.5, 130.5, 132.0, 133.7, 136.0, 138.2, 140.5, 141.8, 146.1, 150.2, 153.9, 156.1, 160.7; $C_{26}H_{20}Br_2N_6O_2$: C 51.34, H 3.31, N 13.82. Found: C 51.30, H 3.20, N 13. 81.

4.3. BACE1 enzymatic assay

The BACE1 enzyme inhibition assay was carried out using a FRET (Forster resonance energy transfer) kit, from Invitrogen (former Pan Vera corporation, Madison, WI) according to the manufacturer instructions. BACE1 (purified baculovirus-expressed enzyme) was diluted with the assay buffer (50 mM sodium acetate, pH 4.5) to make a 3X working solution of 1 Unit/ml. The peptide substrate (Rh-EVNLDAEFK-Quencher) was also diluted with the same assay buffer to provide the 3X stock solution (750 nM). The inhibitor stock solutions in DMSO were diluted with buffer to provide 3X solution of test compounds at different concentrations. The 3X solution of BACE1 enzyme (10 μl) and each inhibitor sample (10 μl) were placed in 96-well plates and gently mixed. The substrate 3X solution (10 μl) was then added to this mixture in each well to start the reaction at the final reaction volume of 30 μl (the final concentration of DMSO in each sample and control wells was equal or less than 4%). The reaction mixtures were incubated at 25 °C for 90 min in the dark and then the reaction was stopped by adding 10 μl of 2.5 mM sodium acetate. Fluorescence was monitored at 544 nm (excitation wave length) and 590 nm (emission wavelength). OM99-2 was used as a reference inhibitor compound. A multi-well spectrofluorometer instrument (BMG LABTECH, Polar star, Germany) was used for measurements. IC_{50} values were calculated with Curve Expert software version 1.34 for Windows. Each experiment was repeated for three to five times. All data were presented as mean ± S.E.M.

4.4. Protection of neuronal PC12 cells against Aβ-induced damage

PC12 (rat pheochromocytoma) cells were a generous gift from Professor Lloyd A. Greene (Department of Pathology and Cell Biology, Columbia University, New York, NY). Cells were grown in monolayer culture on collagen-coated plates at 37 °C in humidified air containing 5% CO_2. Two-thirds of the growth medium was changed every 3–4 days and the cells were sub-cultured once a week. The ability of the synthesized derivatives in protecting neuronal PC12 cells against $A\beta_{25-35}$ induced damage was examined by the MTT assay. Stock solution of $A\beta_{25-35}$ was prepared by dissolution in distilled water to a 0.5 mM concentration. Prior to use, Aβ was diluted in media at a concentration of 55 μM. PC12 cells at a density of 5×10^5 cells/ml (100 μl in each well) were seeded in rat-tail collagen-coated 96-well plates and incubated for 48 h to adhere at 37 °C. Synthesized derivatives at various concentrations were added in triplicate and incubated for 3 h. Human $A\beta_{25-35}$ was then added at a final concentration of 5 μM. After 24 h, 90 μl the medium was taken out and 20 μL of MTT (0.5 mg/ml dissolved in RPMI containing phenol red) was added and incubated for an additional 2 h at 37 °C. Afterwards, formazan crystals were solubilized in 200 μl DMSO. The optical density was measured at 570 nm with background correction at 655 nm using a Bio-Rad microplate reader (Model 680, Bio-Rad). Each experiment was repeated 3–5 times. The percentage of protection was calculated for each compounds based on the equation: Protection of cells (%) = $[(A_0 - A_b)/(100- A_b)] * 100$.

A_0 is the viability% of the cell in the presence of Aβ and derivatives, A_b is the viability % of cells in the presence of Aβ regarded as 0% protection.

4.5. Chelating activity of ferrous (Fe^{2+}) ion

All synthesized compounds were tested for their metal chelating effect using spectroscopic measurements. The chelating effect of the synthesized compounds on ferrous ions was estimated by the method of Dinis with slight modifications [39,40]. Briefly,

100 μL of each test sample (4 mM) was added to 100 μL of 0.6 mM $FeCl_2$. The volume of this solution was increased to 900 μL with methanol. The reaction was initiated by the addition of 100 μL of 5 mM ferrozine into the mixture, which was then left at room temperature for 10 min and followed by measurement of the absorbance at 562 nm [41]. Methanol, Fe^{2+} and ferrozine were used as a control and methanol was used as a sample blank.

4.6. Metal binding studies

The metal binding studies were carried out in a Agilent UV-2450 spectrophotometer in a 1 cm quartz cuvette using mole ratio method [42]. To investigate the metal binding ability of compound, the UV absorption of the 8i (dissolved in DMSO and diluted in MeOH) as best synthetic metal chelator in the absence or presence of $FeSO_4$ was recorded with wavelength ranging from 200 to 800 nm after incubating for 30 min at room temperature [43]. All agents were dissolved in absolute methanol, and the final concentrations of the **8i** were 20 μM and the final concentration of Fe^{+2} ranged from 0 to 80 μM. The stoichiometry of the Fe^{+2}-**8**i complex was determined by titrating the methanol solution of tested compound with ascending of $FeSO_4$.

4.7. Physicochemical parameters

Optimal BACE1 inhibitor compounds should be pharmacologically active and able to enter the CNS. To achieve this, blood brain barrier penetration and physicochemical properties of the target compounds were predicted using the ADMET SAR web-based application at the http://www.scfbio-iitd.res.in/software/drugdesign/lipinski.jsp website.

Acknowledgment

The authors thank the support of the Vice-Chancellor for Research of Shiraz University of Medical Sciences (grant number: 93-6996). This study was part of the PhD thesis of Aida Iraji. We thank Alireza Edraki and Samantha J. Nelson from Umass Medical School, MA, USA for thorough editing of this manuscript.

Appendix A. Supplementary data

Supplementary data related to this article can be found at https://doi.org/10.1016/j.ejmech.2017.09.057.

References

[1] A. Alzheimer's, Alzheimer's disease facts and figures, Alzheimer's Dementia 11 (2015) 332–384.
[2] D.J. Selkoe, J. Hardy, The amyloid hypothesis of Alzheimer's disease at 25 years, EMBO Mol. Med. 8 (2016) 595–608.
[3] J. Hardy, D.J. Selkoe, The amyloid hypothesis of Alzheimer's disease: progress and problems on the road to therapeutics, science 297 (2002) 353–356.
[4] E.T. Parkin, N.T. Watt, I. Hussain, E.A. Eckman, C.B. Eckman, J.C. Manson, H.N. Baybutt, A.J. Turner, N.M. Hooper, Cellular prion protein regulates β-secretase cleavage of the Alzheimer's amyloid precursor protein, Proc. Natl. Acad. Sci. 104 (2007) 11062–11067.
[5] L. Li, X. Zhang, D. Yang, G. Luo, S. Chen, W. Le, Hypoxia increases Aβ generation by altering β- and γ-cleavage of APP, Neurobiol. Aging 30 (2009) 1091–1098.
[6] L. Zhou, N. Brouwers, I. Benilova, A. Vandersteen, M. Mercken, K. Van Laere, P. Van Damme, D. Demedts, F. Van Leuven, K. Sleegers, K. Broersen, C. Van Broeckhoven, R. Vandenberghe, B. De Strooper, Amyloid precursor protein mutation E682K at the alternative β-secretase cleavage β′-site increases Aβ generation, EMBO Mol. Med. 3 (2011) 291–302.
[7] J. Nunan, D.H. Small, Regulation of APP cleavage by α-, β- and γ-secretases, FEBS Lett. 483 (2000) 6–10.
[8] R. Vassar, D.M. Kovacs, R. Yan, P.C. Wong, The beta-secretase enzyme BACE in health and Alzheimer's disease: regulation, cell biology, function, and therapeutic potential, J. Neurosci. Offic. J. Soc. Neurosci. 29 (2009) 12787–12794.
[9] A. Kumar, C.M. Nisha, C. Silakari, I. Sharma, K. Anusha, N. Gupta, P. Nair, T. Tripathi, A. Kumar, Current and novel therapeutic molecules and targets in Alzheimer's disease, J. Formos. Med. Assoc. 115 (2016) 3–10.
[10] A.K. Ghosh, H.L. Osswald, BACE1 ([small beta]-secretase) inhibitors for the treatment of Alzheimer's disease, Chem. Soc. Rev. 43 (2014) 6765–6813.
[11] Y.-C. Yen, A. Kammeyer, K.C. Jensen, A.K. Ghosh, A.D. Mesecar, Development of an efficient structure-based drug discovery platform for BACE1 Inhibitors for the treatment of Alzheimer's Disease, FASEB J. 30 (2016), 607.609-607.609.
[12] R. Vassar, BACE1 inhibitor drugs in clinical trials for Alzheimer's disease, Alzheimer's Res. Ther. 6 (2014) 1.
[13] A. Budimir, Metal ions, Alzheimer's disease and chelation therapy, Acta Pharm. Zagreb. Croat. 61 (2011) 1–14.
[14] M.R. Jones, J.R. Thompson, M.C. Wang, I.J. Kimsey, A.S. DeToma, A. Ramamoorthy, M.H. Lim, T. Storr, Dual-function triazole–pyridine derivatives as inhibitors of metal-induced amyloid-β aggregation, Metallomics Integr. biometal Sci. 4 (2012) 910–920.
[15] M.R. Jones, E.L. Service, J.R. Thompson, M.C. Wang, I.J. Kimsey, A.S. DeToma, A. Ramamoorthy, M.H. Lim, T. Storr, Dual-function triazole-pyridine derivatives as inhibitors of metal-induced amyloid-beta aggregation, Metallomics Integr. biometal Sci. 4 (2012) 910–920.
[16] S.A. James, Q.I. Churches, M.D. de Jonge, I.E. Birchall, V. Streltsov, G. McColl, P.A. Adlard, D.J. Hare, Iron, Copper, and Zinc concentration in abeta plaques in the APP/PS1 mouse model of Alzheimer's disease correlates with metal levels in the surrounding neuropil, ACS Chem. Neurosci. 8 (2017) 629–637.
[17] Z. Sang, X. Qiang, Y. Li, R. Xu, Z. Cao, Q. Song, T. Wang, X. Zhang, H. Liu, Z. Tan, Y. Deng, Design, synthesis and evaluation of scutellarein-O-acetamidoalkylbenzylamines as potential multifunctional agents for the treatment of Alzheimer's disease, Eur. J. Med. Chem. 135 (2017) 307–323.
[18] P. Xu, M. Zhang, R. Sheng, Y. Ma, Synthesis and biological evaluation of deferiprone-resveratrol hybrids as antioxidants, Aβ1–42 aggregation inhibitors and metal-chelating agents for Alzheimer's disease, Eur. J. Med. Chem. 127 (2017) 174–186.
[19] S.-Y. Li, X.-B. Wang, S.-S. Xie, N. Jiang, K.D.G. Wang, H.-Q. Yao, H.-B. Sun, L.-Y. Kong, Multifunctional tacrine–flavonoid hybrids with cholinergic, β-amyloid-reducing, and metal chelating properties for the treatment of Alzheimer's disease, Eur. J. Med. Chem. 69 (2013) 632–646.
[20] J. Jiaranaikulwanitch, P. Govitrapong, V.V. Fokin, O. Vajragupta, From BACE1 inhibitor to multifunctionality of tryptoline and tryptamine triazole derivatives for Alzheimer's disease, Mol. Basel, Switz. 17 (2012) 8312–8333.
[21] M.A. Ansari, S.W. Scheff, Oxidative stress in the progression of alzheimer disease in the frontal cortex, J. Neuropathol. Exp. Neurol. 69 (2010) 155–167.
[22] D. Allan Butterfield, Amyloid β-peptide (1-42)-induced oxidative stress and neurotoxicity: implications for neurodegeneration in Alzheimer's disease brain. A review, Free Radic. Res. 36 (2002) 1307–1313.
[23] M.E. Clementi, S. Marini, M. Coletta, F. Orsini, B. Giardina, F. Misiti, Aβ (31–35) and Aβ (25–35) fragments of amyloid beta-protein induce cellular death through apoptotic signals: role of the redox state of methionine-35, FEBS Lett. 579 (2005) 2913–2918.
[24] T. Nakagawa, H. Zhu, N. Morishima, E. Li, J. Xu, B.A. Yankner, J. Yuan, Caspase-12 mediates endoplasmic-reticulum-specific apoptosis and cytotoxicity by amyloid-[beta], Nature 403 (2000) 98–103.
[25] H. Gurer-Orhan, C. Karaaslan, S. Ozcan, O. Firuzi, M. Tavakkoli, L. Saso, S. Suzen, Novel indole-based melatonin analogues: evaluation of antioxidant activity and protective effect against amyloid β-induced damage, Bioorg. Med. Chem. 24 (2016) 1658–1664.
[26] C. Garino, N. Pietrancosta, Y. Laras, V. Moret, A. Rolland, G. Quéléver, J.-L. Kraus, BACE-1 inhibitory activities of new substituted phenyl-piperazine coupled to various heterocycles: chromene, coumarin and quinoline, Bioorg. Med. Chem. Lett. 16 (2006) 1995–1999.
[27] C. Garino, T. Tomita, N. Pietrancosta, Y. Laras, R. Rosas, G. Herbette, B. Maigret, G. Quelever, T. Iwatsubo, J.L. Kraus, Naphthyl and coumarinyl biarylpiperazine derivatives as highly potent human beta-secretase inhibitors. Design, synthesis, and enzymatic BACE-1 and cell assays, J. Med. Chem. 49 (2006) 4275–4285.
[28] N. Edraki, O. Firuzi, A. Foroumadi, R. Miri, A. Madadkar-Sobhani, M. Khoshneviszadeh, A. Shafiee, Phenylimino-2H-chromen-3-carboxamide derivatives as novel small molecule inhibitors of beta-secretase (BACE1), Bioorg. Med. Chem. 21 (2013) 2396–2412.
[29] N. Edraki, O. Firuzi, Y. Fatahi, M. Mahdavi, M. Asadi, S. Emami, K. Divsalar, R. Miri, A. Iraji, M. Khoshneviszadeh, L. Firoozpour, A. Shafiee, A. Foroumadi, N-(2-(Piperazin-1-yl)phenyl)arylamide derivatives as beta-secretase (BACE1) inhibitors: simple synthesis by ugi four-component reaction and biological evaluation, Arch. Pharm. 348 (2015) 330–337.
[30] L. Zhang, H. Yu, X. Zhao, X. Lin, C. Tan, G. Cao, Z. Wang, Neuroprotective effects of salidroside against beta-amyloid-induced oxidative stress in SH-SY5Y human neuroblastoma cells, Neurochem. Int. 57 (2010) 547–555.
[31] S. Azimi, A. Zonouzi, O. Firuzi, A. Iraji, M. Saeedi, M. Mahdavi, N. Edraki, Discovery of imidazopyridines containing isoindoline-1,3-dione framework as a new class of BACE1 inhibitors: design, synthesis and SAR analysis, Eur. J. Med. Chem. 138 (2017) 729–737.
[32] P.M. Wax, Current use of chelation in american health care, J. Med. Toxicol. 9 (2013) 303–307.
[33] Y. He, P.-F. Yao, S.-b. Chen, Z.-h. Huang, S.-L. Huang, J.-H. Tan, D. Li, L.-Q. Gu, Z.-S. Huang, Synthesis and evaluation of 7,8-dehydrorutaecarpine derivatives as potential multifunctional agents for the treatment of Alzheimer's disease, Eur. J. Med. Chem. 63 (2013) 299–312.

[34] N. Edraki, A. Iraji, O. Firuzi, Y. Fattahi, M. Mahdavi, A. Foroumadi, M. Khoshneviszadeh, A. Shafiee, R. Miri, 2-Imino 2H-chromene and 2-(phenylimino) 2H-chromene 3-aryl carboxamide derivatives as novel cytotoxic agents: synthesis, biological assay, and molecular docking study, J. Iran. Chem. Soc. 13 (2016) 2163–2171.
[35] H. Park, J. Lee, S. Lee, Critical assessment of the automated AutoDock as a new docking tool for virtual screening, Proteins Struct. Funct. Bioinforma. 65 (2006) 549–554.
[36] A. Anand, R.J. Naik, H.M. Revankar, M.V. Kulkarni, S.R. Dixit, S.D. Joshi, A click chemistry approach for the synthesis of mono and bis aryloxy linked coumarinyl triazoles as anti-tubercular agents, Eur. J. Med. Chem. 105 (2015) 194–207.
[37] J.-A. Shin, Y.-G. Lim, K.-H. Lee, Copper-catalyzed azide–alkyne cycloaddition reaction in water using cyclodextrin as a phase transfer catalyst, J. Org. Chem. 77 (2012) 4117–4122.
[38] W. Ried, B. Schleimer, Cyan-acethydrazid zur Darstellung von Stickstoff-Heterocyclen, II. 1-Acyl-3.5-dimethyl-pyrazole als Acylierungsmittel, Angew. Chem. 70 (1958), 164–164.
[39] T.C.P. Dinis, V.M.C. Madeira, L.M. Almeida, Action of phenolic derivatives (acetaminophen, salicylate, and 5-aminosalicylate) as inhibitors of membrane lipid peroxidation and as peroxyl radical scavengers, Arch. Biochem. Biophys. 315 (1994) 161–169.
[40] R. Sudan, M. Bhagat, S. Gupta, J. Singh, A. Koul, Iron (FeII) chelation, ferric reducing antioxidant power, and immune modulating potential of arisaema jacquemontii (Himalayan cobra lily), BioMed Res. Int. 2014 (2014) 7.
[41] M.A. Ebrahimzadeh, S. Nabavl, S. Nabavl, B. Eslami, Antioxidant activity of the bulb and aerial parts of Ornithogalum sintenisii L (Liliaceae) at flowering stage, Trop. J. Pharm. Res. 9 (2010).
[42] P. Xu, M. Zhang, R. Sheng, Y. Ma, Synthesis and biological evaluation of deferiprone-resveratrol hybrids as antioxidants, Aβ 1–42 aggregation inhibitors and metal-chelating agents for Alzheimer's disease, Eur. J. Med. Chem. 127 (2017) 174–186.
[43] Z. Chen, M. Digiacomo, Y. Tu, Q. Gu, S. Wang, X. Yang, J. Chu, Q. Chen, Y. Han, J. Chen, Discovery of novel rivastigmine-hydroxycinnamic acid hybrids as multi-targeted agents for Alzheimer's disease, Eur. J. Med. Chem. 125 (2017) 784–792.